Microscopic structure and multiple charge states of a PtH$_2$ complex in Si

S. J. Uftring, Michael Stavola, P. M. Williams, and G. D. Watkins

Department of Physics, Lehigh University, Bethlehem, Pennsylvania 18015

(Received 21 November 1994)

The structure and electrical properties of a PtH$_2$ complex in Si have been studied by vibrational spectroscopy and electron paramagnetic resonance (EPR). The PtH$_2$ complex has been found to introduce two levels in the Si band gap. One level was identified previously and lies near $E_c - 0.1$ eV. A second, newly discovered level introduced by PtH$_2$ is estimated to lie near midgap. The hydrogen vibrations of the three charge states of PtH$_2$ have been assigned. Electron paramagnetic resonance provides detailed structural information for the paramagnetic charge state and suggests a structure with an off-center Pt$^-$ whose $\langle 001 \rangle$ distortion is reinforced by the pair of hydrogen atoms. An analysis of the small anisotropic part of the hydrogen hyperfine interaction suggests a Pt-H distance of $r \approx 4.2$ Å and helps to locate the positions of the H atoms in the complex.

I. INTRODUCTION

In recent years, there has been much progress made toward understanding hydrogen-passivated shallow impurities in semiconductors.[1,2] Through the interplay between computational theory and experiment, the structures and microscopic properties of many passivated donors and acceptors in elemental and compound semiconductors have been established. However, the hydrogen passivation of deep-level impurities, while discovered earlier, has remained poorly understood.[3] In most previous studies, atomic hydrogen was introduced into thin surface layers that were only a few micrometers thick. This does not lead to a sufficient number of hydrogenated deep centers to study by structure-sensitive methods like electron paramagnetic resonance (EPR) or vibrational spectroscopy because of the low solubility of typical deep-level impurities.

Recently, the introduction of hydrogen into Si at elevated temperature ($\approx 1250\,°C$) has permitted samples to be fabricated with a sufficient number of hydrogenated Pt impurities to be studied by EPR (Refs. 4–7) and infrared (IR) absorption[4,5] spectroscopies. A PtH$_2$ center has been identified by EPR and the hydrogen stretching vibrations of the paramagnetic charge state of this defect complex have been assigned. Surprisingly, it was found that the Pt is not strictly passivated and that the PtH$_2$ center introduces at least one level in the band gap near $E_c - 0.1$ eV (Ref. 4).

In this paper, we report new IR absorption and EPR data for the PtH$_2$ complex. An analysis of the anisotropy of the hydrogen hyperfine interactions provides important new information that helps us to locate the positions of the H atoms in the complex. From uniaxial stress data, we determine the symmetry of the complex that gives rise to the two IR absorption bands previously assigned to the paramagnetic charge state of the PtH$_2$ defect. We then assign the hydrogen vibrations of two additional nonparamagnetic charge states, one that is observed when the Fermi level is above the previously identified level[4] near $E_c = 0.1$ eV and another that is observed when the Fermi level is below a second, newly discovered level introduced by PtH$_2$ that is deep in the gap. In addition to the PtH$_2$ center, there are H vibrations due to other Pt- and H-containing centers in our samples. Results for these additional centers will be discussed briefly.

II. EXPERIMENTAL PROCEDURES

Samples for our experiments were prepared from both n- and p-type Si grown by the floating-zone method. The samples were doped with $[P] = 3 \times 10^{16}$ cm^{-3} and $[B] = 2 \times 10^{15}$ cm^{-1} for the n- and p-type samples, respectively. Pt was introduced by diffusion in sealed quartz ampoules in a He ambient followed by a quench to room temperature in ethylene glycol. From previous solubility data,[8,9] diffusion temperatures of 975 and 1250 °C were selected so as to produce samples with Pt concentrations of 4×10^{15} cm^{-3} and 1×10^{17} cm^{-3}. In the following, we refer to these samples as the low-Pt and high-Pt samples. These Pt concentrations were chosen so that in the low-Pt, n-type samples, the Fermi level would be near the P level at $E_c - 0.045$ eV. In the high-Pt samples the Fermi-level position will be determined by the Pt impurity's deep levels,[9,10] i.e., by the Pt acceptor level at $E_c - 0.23$ eV in n-type starting material and the Pt donor level at $E_v + 0.32$ eV in p-type starting material. These expectations were confirmed for the n-type samples by EPR measurements in which the P resonance (paramagnetic when neutral) was only detected for the low-Pt samples. Diffusion times between 24 and 72 h were used. To introduce H and/or D into the Pt-diffused Si, the samples were subsequently sealed in quartz ampoules with 0.66 atm of H$_2$, D$_2$, or mixtures of both, annealed at 1250 °C for 30 min, and then cooled rapidly to room temperature by removal from the oven.

Infrared absorption measurements were made with a Bomem DA3. 16 Fourier-transform spectrometer that was equipped with a KBr beam splitter and InSb and Hg$_x$Cd$_{1-x}$Te detectors. Spectra were recorded with a resolution of 0.35 cm^{-1}. A 4.5-μm long-pass filter was

inserted before the sample for some of our experiments. For our uniaxial stress experiments, light was polarized with a Molectron wire grid polarizer on a CaF_2 substrate. Stress was applied at low temperature with a push-rod system that was cooled in an Oxford Instruments CF1204 cryostat. Electron-paramagnetic-resonance measurements were performed on a 14 GHz balanced bolometer spectrometer, at 8.5 K in dispersion.

III. PARAMAGNETIC CHARGE STATE OF THE PtH_2 COMPLEX

The paramagnetic charge state of the PtH_2 complex is understood best. Electron-paramagnetic-resonance and IR absorption spectra have been assigned and a structure for the complex has been proposed.[4-7] The new IR and EPR data presented below confirm the previous assignments and help to locate the positions of the hydrogen atoms in the complex.

A. EPR and IR absorption studies of the paramagnetic charge state

In the hydrogenated high-Pt, n-type samples, a new $S = \frac{1}{2}$ EPR spectrum was observed.[4-7] This spectrum was assigned to a PtH_2 complex by the observation of hyperfine interactions with a single ^{195}Pt nucleus ($I = \frac{1}{2}$, 33% abundant) and two equivalent hydrogen nuclei ($I = \frac{1}{2}$, 100% abundant). The change in the hyperfine structure upon the substitution of D ($I = 1$) for H confirmed this assignment. The anisotropy of the g and ^{195}Pt hyperfine tensors showed that the center has C_{2v} symmetry and the model shown in Fig. 1(a) was tentatively proposed for the defect.[4] The rationale for the model was that isolated substitutional Pt^-, which has been extensively studied by EPR,[11] also has C_{2v} symmetry, with the Pt atom displaced off-center toward two of its Si

neighbors. The remaining Si bonds were therefore suggested to be terminated by hydrogen atoms, as shown, retaining the C_{2v} symmetry. In the case of isolated Pt^-, a competition between the energy gain from the off-center distortion and the large Pt spin-orbit interaction, which tends to prevent distortion, has been shown to lead to an intermediate situation where large g shifts and other unusual effects occur.[12] On the other hand, the modest g shifts of the PtH_2 center can be considered fully consistent with the model of Fig. 1(a), where now the presence of the hydrogens aids the off-center distortion sufficiently to suppress the spin-orbit effects. The principal values for the g and ^{195}Pt hyperfine tensors are given in Table I (Ref. 13), and their corresponding axes, 1, 2, and 3, are illustrated in Fig. 1(a).

The new PtH_2 EPR spectrum was observed in the dark only when the Pt concentration was greater than the P concentration, i.e., when the Fermi level was lowered to the Pt acceptor level at $E_c - 0.23$ eV. For a lower Pt concentration, $[Pt] < [P]$, the PtH_2 resonance was only observed under illumination.[4] These results indicated that the PtH_2 defect introduces a level in the gap between the P and Pt levels at $E_c - 0.045$ and 0.23 eV, respectively, and that the complex is only paramagnetic when it is unoccupied. In experiments in which the Fermi-level position was controllably lowered from the P level by successive electron irradiations, the position of the level introduced by PtH_2 was refined further and found to be above $E_c - 0.1$ eV (Ref. 4).

Infrared absorption spectra were measured for the same samples that were used in the EPR experiments and several hydrogen-stretching modes were observed.[4,5] A spectrum is shown in Fig. 2 for a high-Pt sample after the 1250 °C H_2 treatment. The vibrational bands $B1_H$, $B2_H$, $C1_H$, and $C2_H$ decay together upon subsequent annealing and are eliminated together by a 30-min anneal at 600 °C. The PtH_2 EPR signal has very similar annealing behavior. In a variety of samples and under different measurement conditions, the lines $B1_H$ and $B2_H$ always appear with the same relative intensity. Further, when a high-Pt sample was annealed in a mixture of H_2 and D_2, a new band, $B3_H$, appeared (Fig. 2). Taken together, these results led us to assign the bands $B1_H$ and $B2_H$ to the two weakly coupled hydrogen-stretching modes of the paramagnetic charge state of the PtH_2 complex.[4,5] The band $B3_H$ is assigned to the hydrogen-stretching mode of the PtHD complex (in this case, decoupled by the frequency difference between the H and D vibrations) and
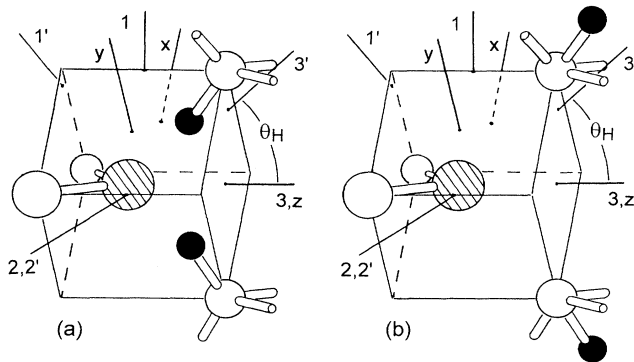

FIG. 1. Tentataive models for the PtH_2 complex in Si. The Pt atom is shown shaded. The H atoms are drawn black. In (a) the weak Si bonds are terminated by H atoms that point toward the Pt atom. In (b) the H atoms point away from the Pt atom. Although the Si atoms are drawn on their lattice sites, there may be substantial relaxations that are not shown. [Our estimate of the Pt-H distance of $r \approx 4.2$ Å determined from the anisotropy of the hydrogen hyperfine interaction favors the model shown in (b).]

TABLE I. Spin-Hamiltonian parameters for the PtH_2 complex in Si. The coordinate axes are shown in Fig. 1. The unprimed coordinates are the principal axes for g and A_{Pt} and the primed coordinates are the principal axes for A_H ($\theta_H = 35°$ in Fig. 1).

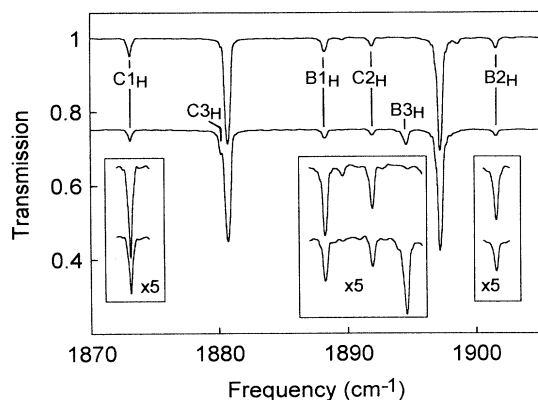|	1 (1')	2 (2')	3 (3')
g	1.9563	2.1683	2.1299
A_{Pt} (MHz)	542	238	172
A_H (MHz)	7.2	8.1	10.9

FIG. 2. Infrared-absorption spectra measured at 4.2 K. The samples are n-type Si into which Pt had been diffused at 1250 °C. The upper spectrum shows the hydrogen-stretching modes for a sample that was annealed in H_2. The lower spectrum shows the hydrogen-stretching modes for a sample that was annealed in a mixture of H_2 and D_2. The insets show vertical expansions of the vibrational bands of the PtH_2 and PtHD complexes.

confirms that $B1_H$ and $B2_H$ are the vibrations of a center that contains two equivalent hydrogen atoms.

There are corresponding vibrational bands in the deuterium-stretching region of the spectrum. Spectra for high-Pt samples that had been annealed in D_2 and in a mixture of H_2 and D_2 are shown in Fig. 3. The bands observed in Fig. 2 all have deuterium-shifted counterparts in Fig. 3. Corresponding bands are labeled similarly with subscripts that indicate whether the band is a H- or D-stretching vibration. Table II contains a list of the hydrogen and deuterium vibrational bands assigned to the PtD_2, PtD_2, and PtHD complexes.

The bands $C1_H$ and $C2_H$ behave very similarly to $B1_H$ and $B2_H$ in the high-Pt, n-type samples and, without fur-
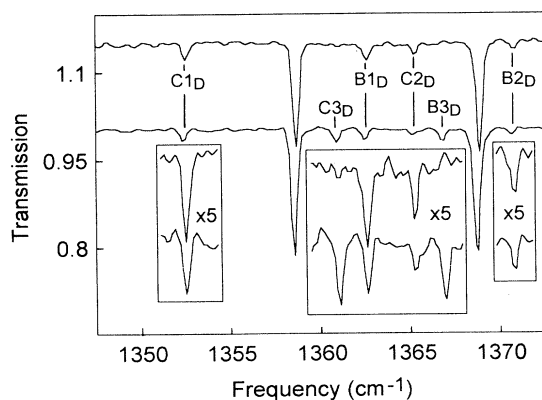
TABLE II. Infrared-absorption bands assigned to the hydrogen vibrations of the different charge states of the PtH_2 complex in Si. The paramagnetic charge state corresponds to $n-1$ with vibrational bands labeled B. There are two additional, non-paramagnetic charge states, $n-2$ and n, with vibrational bands labeled A and C, respectively. Frequencies are given in cm^{-1}.

	$n-2$	$n-1$	n
PtH_2	1889.6 (A1$_H$)	1888.2 (B1$_H$)	1873.1 (C1$_H$)
	1898.0 (A2$_H$)	1901.6 (B2$_H$)	1891.9 (C2$_H$)
PtHD	1893.9 (A3$_H$)	1894.6 (B3$_H$)	1880.3 (C3$_H$)
	1367.5 (A3$_D$)	1366.9 (B3$_D$)	1361.0 (C3$_D$)
PtD_2	1363.3 (A1$_D$)	1362.5 (B1$_D$)	1352.4 (C1$_D$)
		1370.7 (B2$_D$)	1365.2 (C2$_D$)

ther information, are also good candidates for the hydrogen-stretching modes of the paramagnetic charge state. Changes in the spectrum that occur as the Fermi level is varied or under illumination that will be discussed below will confirm our assignments of $B1_H$ and $B2_H$.

B. Location of the hydrogen atoms for the paramagnetic charge state

To probe further the positions of the hydrogen atoms in the model, a careful analysis of the angular dependence of the hydrogen hyperfine interactions has been performed. The results are presented in Fig. 4 for **B** in the 1-3 and 2-3 planes of the defect. These were extracted by matching the observed partially resolved structure of each corresponding branch of the spectrum to a single line shape function convoluted with the four line structure predicted for hyperfine interaction with two $I = \frac{1}{2}$ hydrogens. The branch of the spectrum arising from the defect orientation with **B** in the 2-3 plane is observed to display throughout its angular dependence the well-
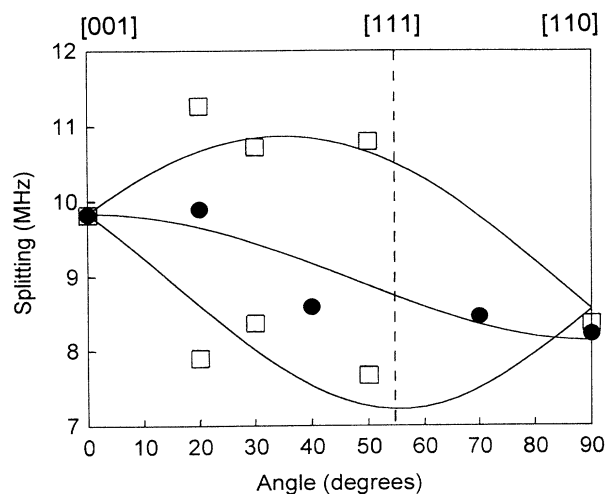

FIG. 3. Infrared-absorption spectra measured at 4.2 K. The samples are n-type Si into which Pt had been diffused at 1250 °C. The upper spectrum shows the deuterium-stretching modes for a sample that was annealed in D_2. The lower spectrum shows the deuterium-stretching modes for a sample that was annealed in a mixture of H_2 and D_2. The insets show vertical expansions of the vibrational bands of the PtD_2 and PtHD complexes.

FIG. 4. Angular dependence of the hydrogen hyperfine interaction. Filled circles are for **B** in the 2-3 plane and open squares are for **B** in the 1-3 plane. (The principal axes are shown in Fig. 1.)
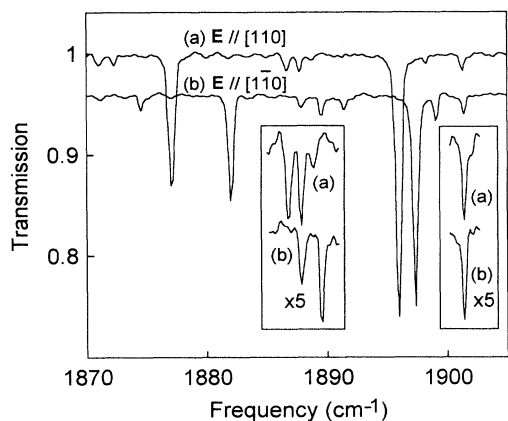
FIG. 5. Infrared-absorption spectra measured near 10 K with a stress of 357 MPa applied along the [110] direction. The propagation direction of the light was k∥[001] and the polarization directions are indicated. The sample was n-type Si into which Pt had been diffused at 1250 °C. The sample was subsequently annealed in H_2 at 1250 °C. The insets show vertical expansions of the stress-split components for bands $B1_H$ (left) and $B2_H$ (right).

Uniaxial stress studies have also been performed for the hydrogen vibrational bands observed in the n-type high-Pt samples. Spectra measured with polarized light for a [110] stress direction and a [001] viewing direction are shown in Fig. 5. (Spectra measured with stress applied along a $\langle 111 \rangle$ axis are shown in Ref. 5.) The behavior of the lines $B1_H$ and $B2_H$ are shown in the insets. In Figs. 6 and 7, the dependence of the stress-split vibrational bands $B1_H$ and $B2_H$, respectively, are shown as a function of the magnitude of the applied stress. The numbers of components, their relative intensities, and their polarization dependencies are consistent with a complex with C_{2v} symmetry, in agreement with the EPR symmetry determination for the paramagnetic charge state. The parameters that were determined from the fits to the data shown in Figs. 6 and 7 are given in Table III. In this analysis, we have followed the treatment of Kaplyanskii[14] where the frequency shift, Δv, for a given defect that is produced by applied stress, σ, is described by the piezospectroscopic tensor, A, for the defect by

$$\Delta v = \mathrm{Tr}(A \cdot \sigma) , \qquad (1)$$

where the components of A are conventionally defined in a cubic axis system for the defect. The results of Table III are given in terms of the defect x, y, z cubic axis system illustrated in Fig. 1, where for C_{2v} symmetry, the nonvanishing components are $A_1 = A_{xx} = A_{yy}$, $A_2 = A_{zz}$, and $A_3 = A_{xy} = A_{yx}$. The directions of the transition moments are also determined from the stress data and differentiate between the $\{110\}$ mirror planes of the PtH_2 complex. Our results show that the transition moment for band $B2_H$ is along the $C_2 - \langle 001 \rangle$ principal axis (z) of the center and for $B1_H$ is along the perpendicular $\langle 110 \rangle$ principal axis (1) that is in the plane that contains the two hydrogen atoms. Thus, $B2_H$ is assigned to the symmetric hydrogen mode and $B1_H$ is assigned to the antisymmetric mode. The $\sim 2:1$ intensity ratio of the antisymmetric to symmetric modes is fully consistent with the projection onto these mode directions of the transition moments of the two individual $\langle 111 \rangle$ Si-H stretching vibrational modes. These results, therefore, further confirm that these are the vibrations of the same PtH_2 center observed by EPR.
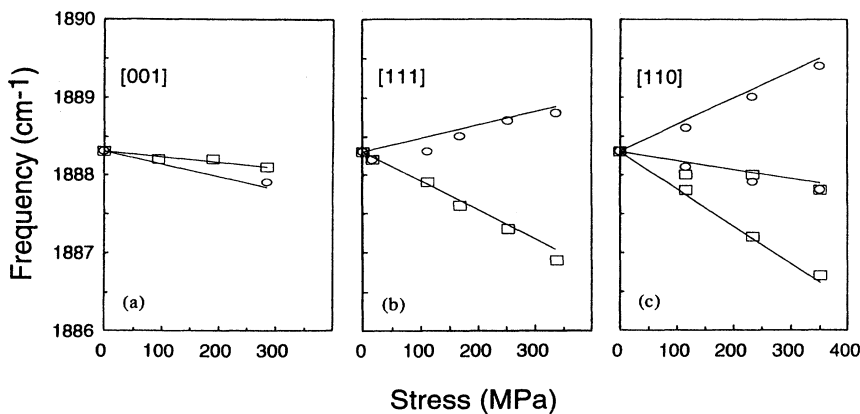
resolved 1:2:1 intensity pattern of a single hyperfine splitting (the filled circles in Fig. 4) associated with each of the two equivalent hydrogen atoms. This confirms the hydrogen locations in the 1-3 plane as originally proposed in the model of Fig. 1(a). For B in the 1-3 plane, the central component displays a partially resolved splitting, revealing the two hydrogens to have different angular dependencies for their hyperfine interactions in this plane (open squares in Fig. 4). A least squares fit to these results leads to the hyperfine tensor components given in Table I with the corresponding principal axes for one of the hydrogen atoms (shown primed) in Fig. 1. The angular dependence of the hyperfine interaction predicted with these values is shown in Fig. 4 as the solid lines. The hyperfine tensor is approximately axially symmetric about directions $\theta_H \approx \pm 35°$ from the $\langle 001 \rangle$ C_2 axis confirming the locations of the hydrogen atoms in the 1-3 plane as approximately in the nearest-neighbor directions from the center.

FIG. 6. Frequency vs the magnitude of the stress applied along the high-symmetry stress directions for the 1888.2 cm^{-1} band ($B1_H$) assigned to the paramagnetic charge state of the PtH_2 complex in Si. The open boxes are for $E\|\sigma$ and the open circles are for $E\perp\sigma$. (For the [110] stress direction, the open circles are for $E\|[1\bar{1}0]$.)
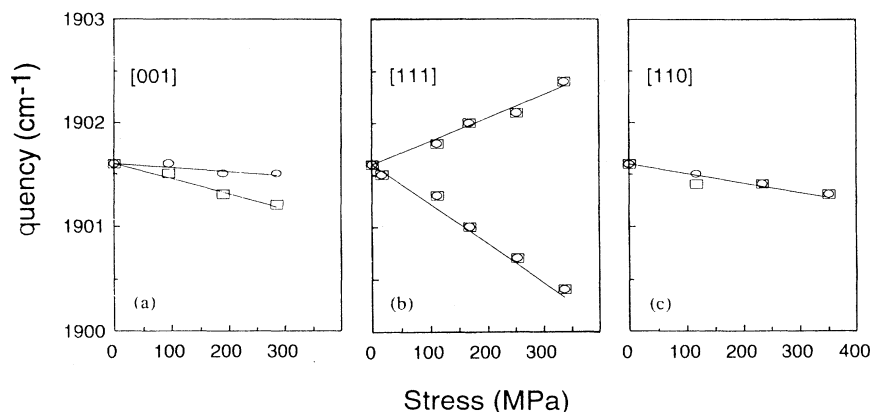
FIG. 7. Frequency vs the magnitude of the stress applied along the high-symmetry stress directions for the 1901.6-cm^{-1} band (B2$_H$) assigned to the paramagnetic charge state of the PtH$_2$ complex in Si. The open boxes are for $E\|\sigma$ and the open circles are for $E\perp\sigma$. (For the [110] stress direction, the open circles are for $E\|[1\bar{1}0]$.)

As was noted when the model shown in Fig. 1(a) was first suggested,[4] the positions of the hydrogen atoms are uncertain, the C_{2v} symmetry requiring only that the two hydrogens lie in one of the {110} planes, symmetrically above and below the other {110} plane. Recently, Jones and co-workers[15] have suggested the structure shown in Fig. 1(b) for the PtH$_2$ complex as an additional possibility based upon their calculations for a similar NiH$_2$ complex. The calculated hydrogen-stretching frequencies for NiH$_2$ complexes with either structure shown in Fig. 1 (Ref. 15) are in reasonable agreement with our data for PtH$_2$, making it difficult to decide between these structures on the basis of the vibrational frequencies alone.

The hydrogen hyperfine interactions can provide further information on this point. Treating the hyperfine tensor as axially symmetric along the 3' axis, we can write,[16]

$$A_{\|}=A_{3'}=a+2b , \tag{2}$$

and

$$A_{\perp}\cong(A_{1'}+A_{2'})/2=a-b , \tag{3}$$

where

$$a=(8\pi/3)g\mu_B g_N\mu_N|\psi(0)|^2 , \tag{4}$$

and

TABLE III. Stress-coupling parameters [following Kaplyanskii (Ref. 14) for a C_{2v} center] determined from the fits to the stress data shown in Figs. 6 and 7 for the 1888.2 and 1901.6 cm^{-1} vibrational bands that have been assigned to the paramagnetic charge state of the PtH$_2$ complex. (The sign of A_3 for the 1901.6 cm^{-1} band cannot be determined from the experiment. However, since we anticipate A to reflect primarily the shifts in the individual Si-H $\langle 111 \rangle$ vibrational frequencies, its sign is assumed to be the same as that for the antisymmetric 1888.2-cm^{-1} band.) Stress-coupling parameters are given in units cm^{-1}/GPa.

	A_1	A_2	A_3
1888.2	-1.6	-0.7	-4.1
1901.6	-1.5	-0.4	$(-)4.5$

$$b=g\mu_B g_N\mu_N\langle(3\cos^2\theta-1)/2r^3\rangle . \tag{5}$$

Here, g and g_N are the electron and nuclear g values, respectively, μ_B and μ_N, the corresponding Bohr magnetons, r, the electron position vector measured from the nucleus, θ, the angle between r and the axis of symmetry, and the brackets in Eq. (5) denote the average over the electronic wave function $\psi(r)$.

The value of $a=8.7$ MHz is only $\sim 0.6\%$ of that for atomic hydrogen (1420 MHz).[17] This is as expected from the model, the unpaired electron wave function for an off-center stabilized Pt$^-$ having a node in the 1-3 plane containing the hydrogens. (Direct evidence for this model of the PtH$_2$ center is also provided by its Pt hyperfine interaction, whose near axial symmetry along the 1-axis identifies it also as reflecting a $d-t_2$ orbital with a node in the 1-3 plane.[12]) The small value for the isotropic term, a, tells us little, therefore, about the Pt-H distance. The anisotropic term, b, on the other hand, can be used as a guide. Since it is small, we approximate it as arising from an electron concentrated at a point r away, at $\theta=0$. In this approximation, our very small value for $b=1.08$ MHz leads to $r\approx 4.2$ Å. This is remarkably close to the expected Pt-H distance of roughly 4.05 Å in the model of Fig. 1(b), which we have estimated to be 2.35 Å, the Si-Si nearest-neighbor distance, plus ~ 1.7 Å, a typical backbond Si-H distance.[18,19] Of course, the electronic wave function is actually spread out, so this close agreement is somewhat fortuitous.[20] Still, considering the r^{-3} dependence, the experimental result for b appears smaller than what one might expect for the model of Fig. 1(a). (An alternative analysis is to take a to be negative, which is equally likely for an atom in the nodal plane, giving 1' for the principal axis of the dipole-dipole interaction. This gives $\theta_H\approx\pm 55°$, closer to the expected $\langle 111 \rangle$ Pt-H direction, but implies greater departure from axial symmetry. In either analysis, however, the value of b is similar and the estimate of the Pt-H distance is essentially unchanged.)

The small anisotropy of the hydrogen hyperfine interactions therefore provides evidence that the PtH$_2$ complex has the configuration shown in Fig. 1(b). However, we still leave open the possibility that a structure similar to that shown in Fig. 1(a) is correct. Jones et al.[15] have

also predicted that the complex of Fig. 1(b) should have a hydrogen wagging mode near 900 cm^{-1} and this has not been observed. For the similar back-bonded structure of donor-hydrogen pairs in Si, the wagging mode is observed easily.[21] Until this question is resolved, we must reserve a definitive conclusion.

IV. VIBRATIONAL SPECTRA OF TWO ADDITIONAL CHARGE STATES OF THE PtH$_2$ COMPLEX

In this section, we will show that in addition to the level at $\sim E_c - 0.1$ eV for the PtH$_2$ center, there is also a level closer to midgap. Therefore, there are three possible charge states of the complex, one of which is paramagnetic (discussed above) and two additional nonparamagnetic charge states. When the charge state of the PtH$_2$ center is changed, either by varying the Fermi-level position or by photoionization, the vibrational frequencies are shifted due to the consequent changes of the defect's force constants.[22] Thus, we can detect and study the additional charge states, even though they are nonparamagnetic, by vibrational spectroscopy.

In the following, we will assign the vibrational modes of the two nonparamagnetic charge states of the PtH$_2$ center. The vibrational bands that will be discussed in this section are also listed in Table II. We will refer to the paramagnetic charge state as PtH$_2^{n-1}$. The more negative charge state that is populated when the Fermi level is above $\approx E_c - 0.1$ eV is then PtH$_2^{n-2}$. The more positive charge state that is populated when the Fermi level is deep in the gap is PtH$_2^n$. In order for the paramagnetic charge state to contain an odd number of electrons, n should be either 0 or 2, which would make the complex a double acceptor or a double donor, respectively.

A. Vibrational modes of a more negative charge state, PtH^{n-2}

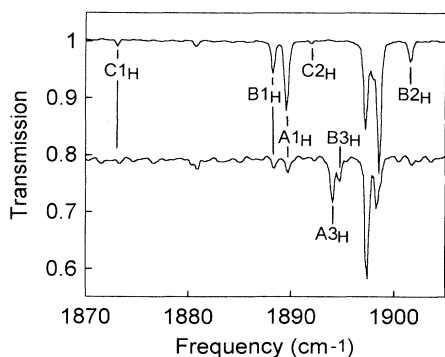In Fig. 8, spectra measured at 4.2 K are shown for low-Pt samples, i.e., with the Fermi level above the level

FIG. 8. Infrared-absorption spectra measured at 4.2 K. The samples are n-type Si into which Pt had been diffused at 975 °C. The upper spectrum shows the hydrogen-stretching modes for a sample that was annealed in H$_2$. The lower spectrum shows the hydrogen-stretching modes for a sample that was annealed in a mixture of H$_2$ and D$_2$.

near $E_c - 0.1$ eV for PtH$_2$. For the sample annealed in H$_2$ (upper spectrum), new bands are observed in addition to bands B1$_H$, and B2$_H$. (C1$_H$, C2$_H$ are also present and are weak.) When the sample temperature is raised to near 40 K, lines B1$_H$ and B2$_H$ disappear and line A1$_H$ increases in intensity. This result suggests that A1$_H$ is a hydrogen mode of the PtH$_2$ complex when it is in its more negative, nonparamagnetic charge state. Band B1$_H$ is present at low temperature because light from the spectrometer photoionizes the PtH$_2$ center and the photogenerated electrons are trapped by the partially compensated P donors at low temperature. At 40 K, the P donor can be thermally ionized and it is no longer an effective trap for the photoionized electrons.

Further support for the assignment of A1$_H$ comes from the effect of illumination on the populations of the different charge states. Filtering the spectrometer light provides a simple and convenient means to vary the illumination conditions and to identify charge-state-sensitive vibrational modes. In our experiments, we have inserted a 4.5-μm (≈ 2220-cm^{-1}) long-pass filter before the sample to eliminate a portion of the spectrometer light (which is outside of our measurement range). Eliminating short-wavelength light from the spectrometer causes the populations of the light-induced charge states to be reduced. Spectra are shown in Fig. 9(a) that were measured with and without the 4.5-μm filter in place. The ratio of these spectra is shown in Fig. 9(b). The changes in the relative intensities of the vibrational bands are clearly seen. In Fig. 9(b), the downward going bands correspond to charge states that would not be populated in darkness, i.e., charge states whose population is reduced when the filter is inserted, and upward going bands correspond to charge states that are depopulated by the spectrometer illumination.
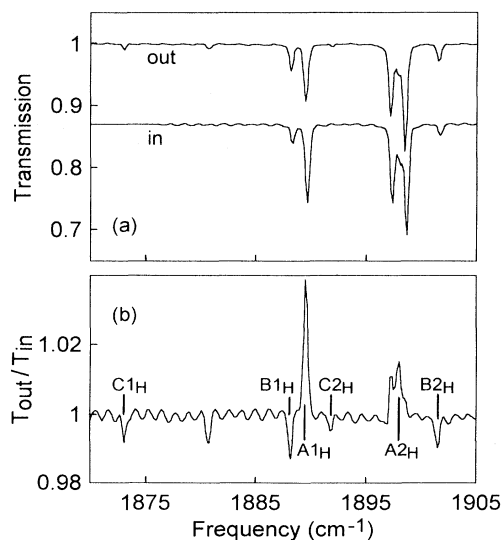

FIG. 9. (a) Infrared-absorption spectra measured at 4.2 K with and without a 4.5-μm long-pass filter placed before the sample. The samples are n-type Si into which Pt had been diffused at 975 °C and that had been subsequently annealed in H$_2$. (b) The ratio of the transmission spectra shown in (a).

Two upward going bands, $A1_H$ and $A2_H$, are apparent in Fig. 9(b). $A1_H$ was suggested above to be a hydrogen mode of the charge state PtH_2^{n-2}. The light-induced intensity changes support this suggestion. $A2_H$ is tentatively assigned to the second hydrogen mode of PtH_2^{n-2} because of its behavior upon illumination. $A2_H$ appears only as a weak shoulder between two stronger unassigned bands in the spectra in Fig. 9(a), but is seen clearly as an upward going band in the ratio shown in Fig. 9(b). Bands $B1_H$ and $B2_H$ are downward going, which suggests that they would not be present in the dark and that they appear at the expense of $A1_H$ and $A2_H$ when the Fermi level is above the PtH_2 level at $E_c - 0.1$ eV.

For an n-type, low-Pt sample annealed in a mixture of H_2 and D_2, new bands due to the PtHD complex appear (lower spectrum in Fig. 8). The weaker of these bands is the decoupled hydrogen-stretching vibration, $B3_H$, of $PtHD^{n-1}$ that was assigned to the paramagnetic charge state in Sec. III above. The other, $A3_H$, is assigned to the decoupled hydrogen vibration of $PtHD^{n-2}$. Similarly, in the deuterium-stretching region of the spectrum, there are the corresponding bands $A1_D$ and $A3_D$ at 1363.3 and 1367.5 cm^{-1}, that are assigned to the deuterium modes of PtH_2^{n-2} and $PtHD^{n-2}$, respectively. The signal to noise ratio in our spectra has not been sufficient for us to identify the band $A2_D^{n-2}$. (The ratio of the frequencies for corresponding H and D stretching modes listed in Table II is $\omega_H / \omega_D \approx 1.386$, which is very close to the value expected for a harmonic Si-H stretching vibration, 1.390. Thus, we expect the band $A2_D^{n-2}$ to be near 1368 cm^{-1} and to be masked by the strong, unassigned band at 1368.8 cm^{-1}.)

B. Vibrational modes of a more positive charge state, PtH_2^n

In Fig. 10, a spectrum is shown for a p-type sample into which Pt and H had been indiffused at 1250 °C. In this case, $[Pt] > [B]$ and the Fermi level in the sample is expected to be near the Pt donor level at $E_v + 0.32$ eV. Only bands $C1_H$ and $C2_H$ appear along with the strong unassigned band at 1880.8 cm^{-1}. In a variety of samples prepared under different conditions, $C1_H$ and $C2_H$ always appear with the same relative intensity. These results

lead us to suggest that there is another nonparamagnetic charge state, PtH_2^n, that is populated when the Fermi level is below an additional level $(n-1)/n$, which must be between the Pt acceptor level at $E_c - 0.23$ eV and the Pt donor level at $E_v + 0.32$ eV. An energy-level diagram is shown in Fig. 11. The bands $C1_H$ and $C2_H$ are assigned to the hydrogen modes of PtH_2^n.

If we reexamine the lower spectrum shown in Fig. 2 that was recorded for a sample that was annealed in a mixture of H_2 and D_2, there is a shoulder observed to the low-frequency side of the strong band at 1880.8 cm^{-1}. Subtraction of the spectra shown in Fig. 2 reveals a band, $C3_H$, at 1880.3 cm^{-1} that we assign to the decoupled hydrogen vibration of $PtHD^n$. The band $C3_D$ observed in the deuterium stretching region that is shown in Fig. 3 (lower spectrum) is assigned to the corresponding decoupled deuterium-stretching mode.

The effect of spectrometer illumination on the populations of the different charge states provides further support for the assignment of lines $C1_H$ and $C2_H$ to a deeper charge state of PtH_2. We begin by noting that bands $C1_H$ and $C2_H$ were present in the spectra for the n-type, high-Pt samples (Fig. 2) and that the deep charge state we have proposed should not have been populated in the dark for these samples (Fermi level near the Pt acceptor level at $E_c - 0.23$ eV). Spectra are shown in Fig. 12(a) that were measured with and without the 4.5-μm filter for the n-type, high-Pt sample. The ratio of these spectra is shown in Fig. 12(b). In this case, the bands $C1_H$ and $C2_H$ are downward going, which shows that they are enhanced by illumination and suggests that they would not be present in the dark. $B1_H$ and $B2_H$ are upward going; hence, the spectrometer illumination is causing the paramagnetic charge state, $n-1$, to be depopulated. These results show that bands $C1_H$ and $C2_H$ appear at the expense of $B1_H$ and $B2_H$ under illumination and fully support our assignment of the former to a more positive, nonparamag-
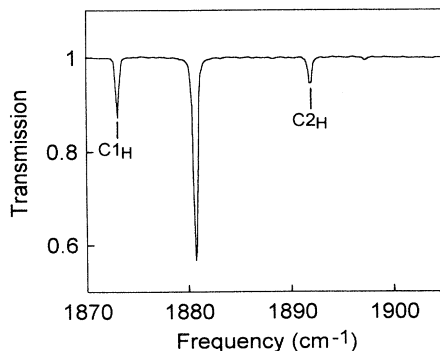

FIG. 10. Infrared-absorption spectrum measured at 4.2 K for a p-type Si sample into which Pt had been diffused at 1250 °C. The sample was subsequently annealed in H_2 at 1250 °C.
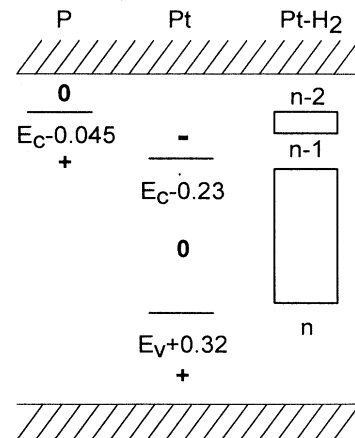

FIG. 11. Energy-level diagram that show the levels of the P, Pt, and PtH_2 defects. The open rectangles indicate that the $(n-2)/(n-1)$ level of the PtH_2 complex is between $E_c - 0.045$ and $E_c - 0.1$ eV and that the $(n-1)/n$ level is between $E_c - 0.23$ and $E_v + 0.32$ eV.
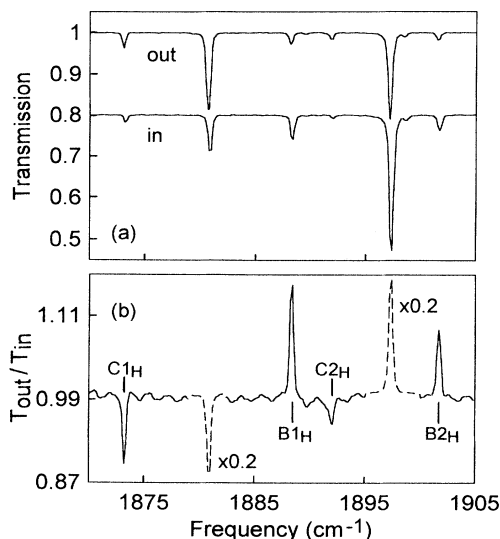
FIG. 12. (a) Infrared-absorption spectra measured at 4.2 K with and without a 4.5-μm long-pass filter placed before the sample. The samples are n-type Si into which Pt had been diffused at 1250 °C and that had been subsequently annealed in H_2. (b) The ratio of the transmission spectra shown in (a). The vertical scale for the vibrational bands drawn with a dashed line has been reduced by a factor of 0.2.

netic charge state, PtH_2^n. Finally, the 4.5-μm filter had no observable effect on the spectrum shown in Fig. 10 for the p-type sample in which the Fermi level is low in the gap. We will comment on this result below.

C. Further comments
on the mode assignments and charge states

The vibrational bands $B1_H$, $B2_H$, $C1_H$, and $C2_H$ decay together upon annealing and are eliminated by a 30 min anneal at 600 °C. These results support our assignment of these bands to the hydrogen vibrations of the same PtH_2 complex in its different charge states. The stronger bands at 1880.8 and 1897.2 cm^{-1} are eliminated together at a slightly higher annealing temperature, 675 °C.

To this point, the absolute charge state of the PtH_2 center has been left uncertain. We know the paramagnetic charge state must have an odd number of electrons so that either PtH_2^- or PtH_2^+ is being seen by EPR. The illumination-induced effects provide a clue to which of these charge states is seen. Under illumination at low temperature, one expects defects in the sample to tend toward their more neutral charge states because the capture radius for a Coulomb capture process is large. For example, donors are expected to have greater electron capture cross sections than acceptors. In our experiments, the illumination of P-doped samples reduces the number of electrons trapped at the PtH_2^{n-2} center suggesting that the EPR active charge state is the acceptor PtH_2^-, i.e., $n = 0$, and that photoionized electrons are preferentially trapped by the P donors. The illumination of B-doped samples (Fermi level near $E_v + 0.32$ eV) does not preferentially ionize PtH_2^n, which is also consistent with this

being an acceptor center that can compete effectively with B for photoionized holes. These results suggest that the PtH_2 center is a double acceptor ($n = 0$ in Fig. 11 and in Table II) and that the charge states that are observed are PtH_2^{2-}, PtH_2^- (paramagnetic), and PtH_2^0.

Our results show that the $(n-1)/n$ level is between the Pt acceptor and donor levels at $E_c - 0.23$ and $E_v + 0.32$ eV, respectively. The electron-electron correlation energy U for isolated transition metals in Si is typically $\sim 0.3 - 0.6$ eV (Refs. 9 and 10). Hence, we expect the $(n-1)/n$ level to be near midgap, i.e., roughly 0.5 eV below the $(n-2)/(n-1)$ level at $\approx E_c - 0.1$ eV.

V. OTHER Pt- AND HYDROGEN-RELATED
VIBRATIONAL BANDS

There are a number of hydrogen-stretching bands observed in our spectra that have not been assigned. For example, there are the strong features at 1880.8 and 1897.2 cm^{-1} observed in the spectra shown in Fig. 2 for the high-Pt, n-type samples. (The correspnding bands in deuterated samples are at 1358.5 and 1368.8 cm^{-1} in Fig. 3.) The intensities of these bands are not well correlated to the bands assigned to the PtH_2 complex and are presumably associated with an additional complex (or complexes) that contains Pt and hydrogen. There are no additional new bands related to the 1880.8 and 1897.2 cm^{-1} bands in samples annealed in a mixture of H_2 and D_2, suggesting that each involves the vibration of a single hydrogen atom. In the ratio of the spectra measured with and without the 4.5-μm filter shown in Fig. 12(b), the 1880.8-cm^{-1} band is downward going, whereas the 1897.2-cm^{-1} band is upward going which suggests that the 1880.8-cm^{-1} band would not be present in the dark and appears at the expense of the 1897.2-cm^{-1} band. Further, the 1897.2-cm^{-1} band is relatively more intense in the spectrum shown in Fig. 8 for the low-Pt, n-type sample (Fermi level near $E_c - 0.23$ eV) and only the 1880.8-cm^{-1} band is present in the spectrum shown in Fig. 10 for the Pt-diffused, p-type sample (Fermi level near $E_v - 0.32$ eV). These results all suggest that the 1880.8 and 1897.2 cm^{-1} bands are associated with different charge states of the same defect. Finally, the 1897.2 cm^{-1} band gives rise to a splitting pattern under stress that is characteristic of an A_1 mode of a trigonal center. The 1880.8 cm^{-1} band shows a more complicated behavior under stress that we are continuing to investigate.

In the low-Pt, n-type sample, there is an additional band observed at 1898.6 cm^{-1} (Fig. 8), which we previously speculated[4] might be due to a different charge state of the same complex that gives rise to the 1897.2 cm^{-1} band. The changes in the intensities of these bands, when the 4.5-μm filter is placed before the sample, do not support this interpretation, i.e., one band does not appear at the expense of the other in Fig. 9(b). Hence the 1898.6-cm^{-1} band appears to be due to still another center that contains Pt and H.

In Pt-diffused samples that were rapidly quenched in ethylene glycol following the anneal in H_2, several additional hydrogen-stretching bands were observed. Bands

that have been observed in several samples lie at 1905.9, 1914.2, 1918.0, and 1921.9 cm^{-1}. An anneal at 400 °C eliminates these bands and shows that the complexes that give rise to them are less thermally stable than the PtH$_2$ complex. Their lower stability explains why these bands are only observed in samples that have received a rapid quench following the hydrogen indiffusion.

VI. CONCLUSION

The combination of EPR and IR adsorption spectroscopies has provided detailed information about the microscopic structure and electrical characteristics of a PtH$_2$ complex in Si. The conventional wisdom[3] had been that when hydrogen forms a complex with a transition metal impurity, the gap is swept clean of states. (Exceptions are provided by recent work in which deep-level transient spectroscopy peaks have been observed in Si that contained a transition-metal impurity and hydrogen that had been introduced at low temperature.[23-25]) For the PtH$_2$ center, we have shown that there are two levels, one near the conduction band[4] and a second close to midgap.

Of the three possible charge states for PtH$_2$, only one is paramagnetic. Both EPR (Refs. 4–7) and the stress-induced splittings of the hydrogen vibrational bands show that the PtH$_2$ complex has C_{2v} symmetry in its paramagnetic charge state. The near axial symmetry of the ^{195}Pt hyperfine tensor and the very small isotropic component of the hydrogen hyperfine interaction provide evidence for a structure with an off-center Pt$^-$ whose $\langle 001 \rangle$ distortion is reinforced by the nearby hydrogen atoms. The anisotropy of the hydrogen hyperfine interaction indicates which of the $\{110\}$ planes of the defect contains the two equivalent hydrogen atoms. The directions of the vibrational transition moments determined from the uniaxial stress data lead to the assignment of the band at 1888.2 cm^{-1} to the antisymmetric hydrogen vibration and the band at 1901.6 cm^{-1} to the symmetric vibration. The transition moment directions also link the vibrational transitions to the principal axes of the g and hyperfine tensors determined by EPR.

Vibrational spectroscopy is not limited to the paramagnetic charge state of the PtH$_2$ complex. The changes in the vibrational frequencies that occur when the charge state of the PtH$_2$ defect is changed, either by a shift of the Fermi level or by photoionization, help to locate the levels of the defect and have led to an assignment of the hydrogen vibrations of all three charge states. There are three pairs of hydrogen vibrational bands, one pair for each of the different charge states of the PtH$_2$ center. (There are also three pairs of bands for PtD$_2$ and three

pairs of bands for PtHD.) It has been argued that the PtH$_2$ defect is a double acceptor and that the charge states that have been observed are PtH$_2^{2-}$, PtH$_2^-$ (paramagnetic), and PtH$_2^0$.

The availability of data that provides structural information for a transition-metal-hydrogen complex should help to advance theory in the area. We had suggested that the hydrogen atoms terminate two weak bonds that point toward the off-center Pt atom.[4] Recent calculations by Jones et al.[15] suggest an alternative structure as an additional possibility in which the hydrogen atoms are attached to the Pt atom's Si neighbors at back-bonding sites and point away from the Pt atom. Both of these structures are consistent with the C_{2v} symmetry of the defect. Here, we have found that an analysis of the small anisotropic part of the hydrogen hyperfine interaction leads to an estimate of the Pt-hydrogen distance that is close to that suggested by the structural model of Jones et al. with the hydrogen atoms at the back-bonded sites.

In addition to the PtH$_2$ complex, the hydrogen vibrations of several unidentified centers that presumably contain Pt and hydrogen have been observed in our samples. These defects are the subject of continuing work in our laboratory.

Note added in proof. In recent experiments [M. Evans and M. Stavola (unpublished)], we have found that a stress-induced dichroism (difference in the absorption coefficients measured with light beams polarized parallel and perpendicular to the applied stress direction) is produced by stresses applied along [111] and [110] directions at elevated temperatures for the 1880.8- and 1897.2-cm^{-1} vibrational bands that we have observed in Si that contains Pt and H. The dichroism persists when the stress is removed near 4 K and anneals away for both bands together near 40 K. The similarity of the annealing kinetics for the stress-induced dichroism for the 1880.8- and 1897.2-cm^{-1} bands suggest that they arise from one defect that can be aligned by stress and supports the suggestion made in Sec. V that they are due to two different charge states of the same defect.

[1]S. J. Pearton, J. W. Corbett, and M. Stavola, *Hydrogen in Crystalline Semiconductors* (Springer-Verlag, Berlin, 1992).

[2]*Hydrogen in Semiconductors,* edited by J. I. Pankove and N. M. Johnson (Academic, San Diego, 1991).

[3]See, for example, S. J. Pearton, J. W. Corbett, and M. Stavola,

in *Hydrogen in Crystalline Semiconductors* (Ref. 1), Chap. 3 or S. J. Pearton, *Hydrogen in Semiconductors* (Ref. 2), Chap. 5.

[4]P. M. Williams, G. D. Watkins, S. Uftring, and M. Stavola, Phys. Rev. Lett. **70**, 3816 (1993).

[5]P. M. Williams, G. D. Watkins, S. Uftring, and M. Stavola, in

Defects in Semiconductors 17, edited by H. Heinrich and W. Jantsch (Trans Tech, Zürich, 1994), p. 891.

[6]M. Höhne, U. Juda, Yu. V. Martynov, T. Gregorkiewicz, C.A. J. Ammerlaan, and L. S. Vlasenko, in *Defects in Semiconductors 17* (Ref. 5), p. 1659.

[7]M. Höhne, U. Juda, Yu. V. Martynov, T. Gregorkiewicz, C. A. J. Ammerlaan, and L. S. Vlasenko, Phys. Rev. B **49**, 13 423 (1994).

[8]K. P. Lisiak and A. G. Milnes, Solid State Electron. **18**, 533 (1975).

[9]*Impurities and Defects in Group IV Elements and III-V Compounds,* edited by O. Madelung and M. Schulz, Landolt-Börnstein, New Series, Group III, Vol. 22, Pt. b (Springer, Berlin, 1989), p. 283.

[10]H. Fechtinger, in *Electronic Structure and Properties of Semiconductors,* edited by W. Schröter (VCH, Weinheim, 1991), p. 143.

[11]F. G. Anderson, R. F. Milligan, and G. D. Watkins, Phys. Rev. B **45**, 3279 (1992).

[12]F. G. Anderson, F. S. Ham, and G. D. Watkins, Phys. Rev. B **45**, 3287 (1992).

[13]As was pointed out by Höhne *et al.* in Ref. 7, one of the components of A_{Pt} was reported incorrectly by us in Ref. 4.

[14]A. A. Kaplyanskii, Opt. Spektrosk. **16**, 606 (1964) [Opt. Spectrosc. (USSR) **16**, 329 (1964)].

[15]R. Jones, A. Resende, S. Öberg, J. Goss, and P. R. Briddon (unpublished); R. Jones (private communicator).

[16]G. D. Watkins and J. W. Corbett, Phys. Rev. **121**, 1001 (1961).

[17]N. F. Ramsey, *Nuclear Moments* (Wiley, New York, 1953), p. 89.

[18]S. B. Zhang and D. J. Chadi, Phys. Rev. B **41**, 3882 (1990).

[19]P. J. H. Denteneer, C.G. Van de Walle, and S. T. Pantelides, Phys. Rev. B **41**, 3885 (1990).

[20]The hyperfine interaction for a $5d$ electron on a free ^{195}Pt atom has an estimated value of $b = 364$ MHz [A. K. Koh and D. J. Miller, At. Data Nucl. Tables **33**, 235 (1985)]. From Table I, the value of b for the PtH$_2$ defect, $\sim \frac{1}{3}[A_1 - (A_2 + A_3)/2] = 112$ MHz, corresponds, therefore, to only $\sim 31\%$ localization in the $5d$ shell of the Pt. Hohne *et al.* (Ref. 7), with a stronger EPR signal, were able to detect weak hyperfine satellites arising from ^{29}Si neighbors, and estimated an additional 26% of the wave function distributed equally between two Si neighbors.

[21]K. Bergman, M. Stavola, S. J. Pearton, and J. Lopata, Phys. Rev. B **37**, 2770 (1988).

[22]R. C. Newman, *Infrared Studies of Crystal Defects* (Taylor & Francis, London, 1973). See, for example, the discussion of irradiation damage in silicon on p. 117 and the discussion of the oxygen-vacancy center that follows.

[23]E. Ö. Sveinbjörnsson and O. Engström, Appl. Phys. Lett. **61**, 2323 (1992).

[24]E. Ö. Sveinbjörnsson, G. I. Andersson, and O. Engström, Phys. Rev. B **49**, 7801 (1994).

[25]T. Sadoh, M. Watanabe, H. Nakashima, and T. Tsurushima, in *Defects in Semiconductors 17* (Ref. 5), p. 939.